Journal of Photochemistry and Photobiology B: Biology 140 (2014) 249–254

Contents lists available at ScienceDirect

Journal of Photochemistry and Photobiology B: Biology

journal homepage: www.elsevier.com/locate/jphotobiol

Faster recovery of a diatom from UV damage under ocean acidification

Yaping Wu [a], Douglas A. Campbell [b], Kunshan Gao [a,*]

[a] State Key Laboratory of Marine Environmental Science, Xiamen University, Xiamen, China
[b] Biology Department, Mount Allison University, Sackville, New Brunswick, Canada

ARTICLE INFO

Article history:
Received 11 June 2014
Received in revised form 4 August 2014
Accepted 7 August 2014
Available online 20 August 2014

Keywords:
Ocean acidification
Ocean stratification
Photoinhibition
Photosystem II
UV radiation

ABSTRACT

Diatoms are the most important group of primary producers in marine ecosystems. As oceanic pH declines and increased stratification leads to the upper mixing layer becoming shallower, diatoms are interactively affected by both lower pH and higher average exposures to solar ultraviolet radiation. The photochemical yields of a model diatom, *Phaeodactylum tricornutum*, were inhibited by ultraviolet radiation under both growth and excess light levels, while the functional absorbance cross sections of the remaining photosystem II increased. Cells grown under ocean acidification (OA) were less affected during UV exposure. The recovery of PSII under low photosynthetically active radiation was much faster than in the dark, indicating that photosynthetic processes were essential for the full recovery of photosystem II. This light dependent recovery required *de novo* synthesized protein. Cells grown under ocean acidification recovered faster, possibly attributable to higher CO_2 availability for the Calvin cycle producing more resources for repair. The lower UV inhibition combined with higher recovery rate under ocean acidification could benefit species such as *P. tricornutum*, and change their competitiveness in the future ocean.

1. Introduction

In the modern ocean, marine organisms are affected by interacting factors, including ocean acidification (OA) and UV radiation exposures [1]. The global decline of oceanic pH induced by human activity [2] is altering the chemistry of seawater [3] and affecting most marine organisms directly or indirectly [4–6]. Calcifying organisms show lower calcification [7], diatoms may become more sensitive to high light under OA [8], while fishes may lose their way home [9]. pH is already highly variable in coastal areas because of biological activities or riverine input [13]; upwelled seawater from deep layers are usually acidified with higher pCO_2 [14]. In parallel phytoplankton are exposed to changing intensities and spectra of solar light due to physical mixing, weather conditions, and seawater properties [18–20]. The UV radiation component of sunlight (UV, 280–400 nm) affects biological processes [10,11] down to 60 m in pelagic waters, while UV penetration in coastal areas varies depending on regional optical properties of seawater [12].

Phytoplankton cells are therefore already affected by changing exposures to UV and high CO_2/low pH [11]. UV can synergistically lower photosynthetic rates of phytoplankton under OA [15,16]; but in contrast, a model diatom was less inhibited by UV due to a higher repair rate under OA [17]. While fluctuating solar light can mitigate UV inhibition, and even enhance primary production compared with phytoplankton under Photosynthetically Active Radiation (PAR) alone [21,22].

Photosystem II (PSII) is the enzyme complex that converts light energy to metabolically available electrons [23]. PSII is susceptible to damage by high light or UV radiation [24], with its subunits being damaged and disassembled [25,26]. Therefore, maintenance and repair of PSII is essential for sustained photosynthetic carbon fixation by the Calvin cycle [27]. The Calvin cycle in turn affects the performance of PSII, as the interruption of CO_2 fixation led to faster net photoinactivation of PSII [28]. Increased CO_2 availability and hence a higher carbon fixation rate might facilitate the repair of damaged PSII [17].

Diatoms are the most abundant phytoplankton in the ocean, contributing 20% of global primary productivity [29], and thus have significant influences on carbon export and the marine ecosystem due both to their abundance and their wide cell size distribution [30]. Diatoms are affected by ocean acidification and UV radiation, with their photosynthesis and growth being stimulated by OA at low or moderate light [31], but inhibited by UV radiation [32]. Recent studies revealed that some diatoms, such as *Thalassiosira pseudonana*, are more sensitive to UV radiation under higher CO_2 levels [15], while antagonistic effects of OA and UVB were observed

* Corresponding author.
E-mail address: ksgao@xmu.edu.cn (K. Gao).

http://dx.doi.org/10.1016/j.jphotobiol.2014.08.006
1011-1344/

in *Phaeodactylum tricornutum* [17]. However, the underlying mechanisms for these responses are still unclear.

Considering the increased CO_2 availability under OA conditions and thus potentially higher photosynthesis, we hypothesized that a diatom grown under OA condition would be able to produce more resources for the repair of PSII units, thereby mitigating the effects of UV inhibition and accelerating the recovery rate after UV exposure.

2. Materials and methods

2.1. Species, culture conditions and seawater carbonate system

P. tricornutum (CCMA 106) was isolated from the South China Sea (SCS) in 2004 and obtained from the Center for Collections of Marine Bacteria and Phytoplankton (CCMA) of the State Key Laboratory of Marine Environmental Science (Xiamen University). The cells were inoculated in artificial seawater prepared according to Aquil medium [33], then enriched with 100 μmol nitrate kg^{-1}, 10 μmol phosphate kg^{-1} and 100 μmol silicate kg^{-1}. Target pH (pCO_2) in the cultures and in the fresh medium were achieved by bubbling pre-mixed air-CO_2 mixtures at 388 or 1000 ppmv within a plant growth CO_2 chamber (HP1000G-D, Ruihua), which controls the high CO_2 level with a variation of less than 30 ppmv. The pH changes were determined with a pH meter (Benchtop pH510, OAKTON) which was calibrated with standard National Bureau of Standards (NBS) buffer solution (Hanna), the parameters of carbonate system were computed with CO_2SYS software (Table 1).

Cultures were maintained semi-continuously for at least 20 generations under 2 levels of pCO_2 before used for experiments. Approximately 70% culture volume was renewed with pre-equilibrated medium every 24 h to maintain a stable carbonate system and the cell suspension densities within a range of 8×10^4–3×10^5 cells mL^{-1}. The cultures were illuminated with cool white fluorescent tubes at photon flux densities of 120 μmol m^{-2} s^{-1} (14: 10 light: dark) and 20 °C. Cell concentration was measured every 24 h with particle count and size analyzer (Z2 Coulter, Beckman) before and after dilution with fresh medium. The specific growth rate (μ, d^{-1}) was calculated as: $\mu = (\mathrm{Ln}\ C_2 - \mathrm{Ln}\ C_1)/(T_2 - T_1)$, where C_1 and C_2 represent the cell concentrations at T_1 (after dilution) and T_2 (before dilution).

2.2. Experimental treatments

In the middle of the light period (6–8 h after the light turned on), cells were gently filtered onto polycarbonate membrane, then re-suspended in 20 mmol Tris L^{-1} buffered seawater medium (pH 7.80 or pH 8.15) with a final cell density of ~3×10^4 mL^{-1}. These cell suspensions were transferred into a quartz tube (50 mL), and covered with Schott filters WG295 or WG 395 that block the radiation below 295 or 395 nm, to create PAR + UV and PAR treatments. The cuvettes were then incubated in a water bath under a solar simulator (Sol 1200 W; HÖnle) at growth (PAR: 27 W m^{-2} or 130 μmol m^{-2} s^{-1}, UV: 5.93 W m^{-2}, corresponding to a depth of ~30 m in South China Sea [34]) or higher light levels (PAR: 145 W m^{-2} or 696 μmol m^{-2} s^{-1}, UV: 35.9 W m^{-2}, corresponding to a depth of ~3.7 m in South China Sea [34]) for 1 h. Water temperature was maintained with a cooling system (CTP-3000, Eyela). Before and during the light exposure, fluorescence was measured with a fast induction and relaxation system (FIRe, Satlantic) at time intervals of 30 min (*see* below).

To examine the recovery process of UV-damaged cells under darkness-low light or low light due to different mixing depth, cultures that had been incubated (*see* above) under the PAR + UV treatments for 1 h were then treated with a final concentration of 200 μg chloramphenicol mL^{-1} (or the same volume of ethanol solvent as control) and covered with aluminum foil in darkness for 60 min before transferred to low PAR (13 W m^{-2} or 62.4 μmol m^{-2} s^{-1}, corresponding to a depth of ~43 m in South China Sea [34]) for 30 min, or moved to low PAR directly.

Table 1
Parameters of the seawater carbonate system under the ambient and enriched CO_2 levels. Data are the means ± SD of 9 measurements.

Parameter	380 ppmv	1000 ppmv
pH	8.16 ± 0.04	7.74 ± 0.02
DIC (μmol kg^{-1})	2168 ± 8	2300 ± 13
HCO_3^- (μmol kg^{-1})	1889 ± 29	2153 ± 5
CO_3^{2-} (μmol kg^{-1})	268 ± 31	116 ± 7.3
CO_2 (μmol kg^{-1})	10.5 ± 1.6	31.3 ± 2.1

2.3. Chlorophyll fluorescence measurements

Photochemical yield (Φ_{PSII}) was measured with the FIRe (Satlantic, Halifax, Canada) (Figs. 2–4) or XE-PAM instruments (Walz, Germany) (Fig. 5) while the functional cross section area of PSII (σ_{PSII}) was measured with the FIRe. The duration and intensity of the single turnover flash light for the FIRe was 80 μs at 46000 μmol m^{-2} s^{-1}, while the saturation pulse applied for PAM was 0.8 s at 5000 μmol m^{-2} s^{-1}.

2.4. Data analysis

Φ_{PSII} measured with XE-PAM was determined on the basis of the maximal fluorescence (F_m) and the steady-state fluorescence (F_t) of the light (or dark)-adapted cells, calculated as:

$$(F_m - F_t)/F_m$$

Φ_{PSII} and σ_{PSII} measured with FIRe were determined from fluorescence induction curves processed with MATLAB software using the Fireworx program [35], with specific lamp calibration factors provided by the manufacturer (Satlantic).

The PSII electron transport rate (ETR) (e^- $PSII^{-1}$ s^{-1}) was estimated as:

$$\mathrm{ETR} = \mathrm{PFD} \times \sigma_{PSII} \times q_P \times A,$$

where PFD is the photon flux density (μmol m^{-2} s^{-1}), σ_{PSII} is the functional absorbance cross section of PSII under incubation light levels, q_P is the approximate fraction of PSII open under incubation light, while A converts photons absorbed by PSII to electrons, for details *see* Wu et al. [38].

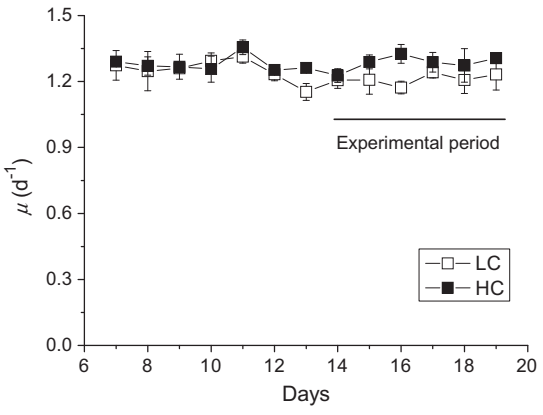

Fig. 1. The growth rate of LC and HC cells during acclimation (before day 14) and experimental periods (day 14–19), vertical bars represent standard deviation, $n = 3$.

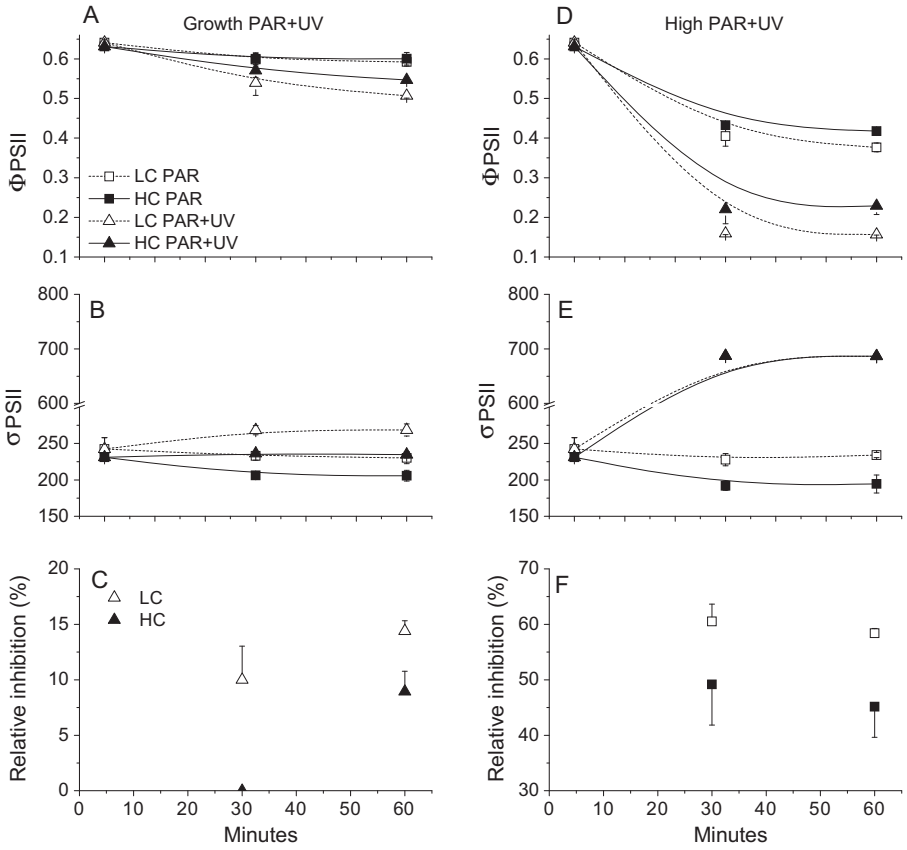

Fig. 2. Photochemical yield (Φ_{PSII}) (A) and functional absorption cross section (σ_{PSII}) (B) of LC and HC grown cells before (i.e. dark adapted) and after PAR (27 W m^{-2}) or PAR + UV (27, 5.6 W m^{-2}) exposure, and the relative UV inhibition, (C) on photochemical yield after 30 or 60 min; Φ_{PSII} (D) and σ_{PSII} (E) of LC and HC grown cells before (i.e. dark adapted) and after PAR (145 W m^{-2}) or PAR + UV (145, 35.9 W m^{-2}) exposure, and the relative UV inhibition (F) on photochemical yield after 30 or 60 min, vertical bars represent standard deviation, $n = 3$ (triplicate cultures).

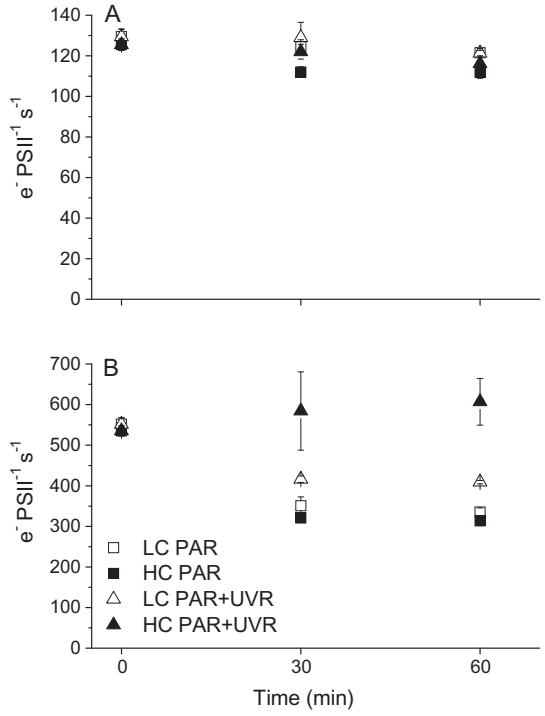

Fig. 3. The PSII electron transport rate (e$^-$ PSII^{-1} s^{-1}) of LC and HC grown cells under growth PAR or PAR + UV (A) and elevated PAR or PAR + UV (B) conditions, vertical bars represent standard deviation, $n = 3$.

The relative inhibition of UV radiation on PSII was calculated as below:

$$\mathrm{Inh_{UV}} = (\Phi_{PSII(PAR)} - \Phi_{PSII(PAB)})/\Phi_{PSII(PAR)} \times 100\%$$

where $\Phi_{PSII(PAR)}$ and $\Phi_{PSII(PAB)}$ represent photochemical yields under PAR and PAB (PAR + UV) treatments, respectively.

The recovery rate of PSII, dependent upon protein-synthesis under low light, was calculated from linear fitting for the first 40 min under low light, after subtracting NPQ relaxation in the dark. Statistical differences among treatments were tested with one-way ANOVA with significance level set at $p = 0.05$.

3. Results

The growth rate of LC (low CO_2) and HC (high CO_2) grown cells was similar during culturing, around 1.26 d^{-1}, experiments were carried out at day 14–19 (Fig. 1). The major parameters of carbonate system are shown in Table 1, pH of LC culture was around 8.16, while HC was around 7.74. The aqueous CO_2 concentration of LC was around 1/3 of HC.

The dark adapted photochemical yields (Φ_{PSII}) were around 0.64 for LC grown cells and for HC (Fig. 2A) grown cells. After exposure to growth PAR (27 W m^{-2}) for 30 min, Φ_{PSII} (light adapted photochemical yield) to around 0.60 for both LC and HC, with no further change for the subsequent 30 min exposure (Fig. 2A). Over 60 min exposure to growth PAR + UV (27, 5.93 W m^{-2}), Φ_{PSII} of LC cells decreased to 0.51 ($p < 0.01$), while Φ_{PSII} of HC cells decreased to 0.55 ($p < 0.001$) (Fig. 2A). The dark adapted σ_{PSII} were around 240 A^2 PSII^{-1} for LC grown cells and 230 A^2 PSII^{-1} for HC grown

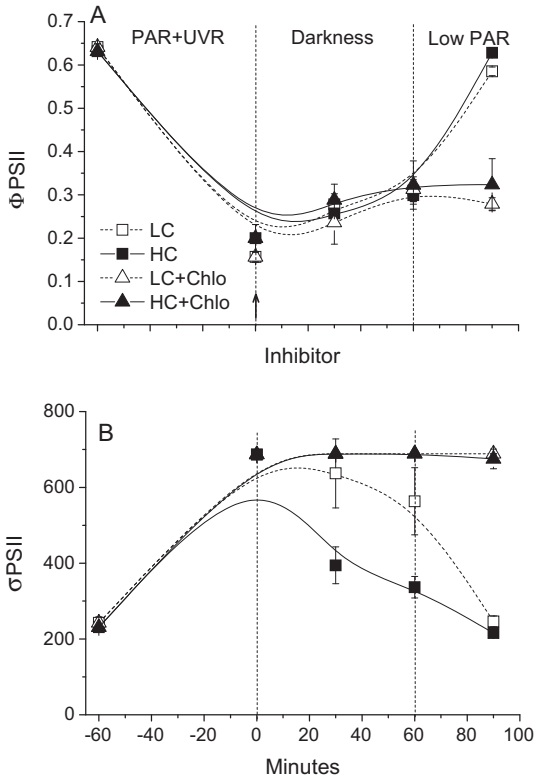

Fig. 4. The time series of Φ_{PSII} (A) and σ_{PSII} (B) of LC and HC grown cells during 1 h exposure to PAR + UV (145, 35.9 W m^{-2}), and the changes of Φ_{PSII} and σ_{PSII} after subsequent 30 min darkness or low light (13 W m^{-2}), cells were treated with or without chloramphenicol (chlo) at the end of PAR + UV exposure, vertical bars represent standard deviation, n = 3.

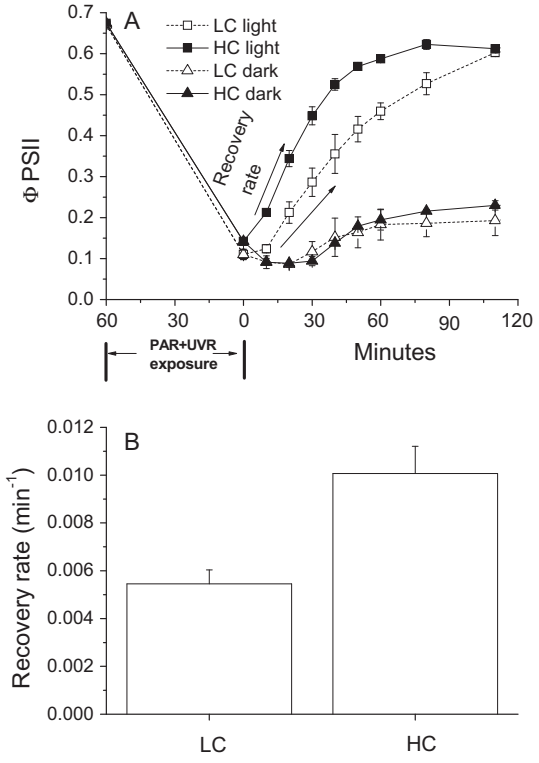

Fig. 5. Φ_{PSII} of LC and HC cells before and after 60 min exposure to PAR + UV (145, 35.9 W m^{-2}), and during the subsequent recovery under low light (13 W m^{-2}) or darkness for 110 min (A), and the recovery rates of LC and HC cells under low light, vertical bars represent standard deviation, n = 3.

cells. σ_{PSII} decreased after growth PAR exposure (Fig. 2B), but σ_{PSII} increased after growth PAR + UV ($p < 0.01$) (Fig. 2B). The relative inhibition induced by UV on photosystem II quantum yield was 15% for LC but only 9% for HC grown cells after 60 min of growth PAR + UV exposure (Fig. 2C). After 60 min exposure to high PAR (145 W m^{-2}), Φ_{PSII} decreased to 0.38 for LC grown cells and 0.42 for HC grown cells ($p < 0.001$) (Fig. 2D), while under high PAR + UV (145, 35.9 W m^{-2}), Φ_{PSII} decreased to 0.16 for LC grown cells and 0.22 for HC grown cells ($p < 0.001$) (Fig. 2D). σ_{PSII} of both LC and HC grown cells decreased after exposure to high PAR ($p < 0.05$), but increased to ~680 A^2 PSII^{-1} after exposure to PAR + UV ($p < 0.001$) (Fig. 2E). The relative UV inhibition of Φ_{PSII} was around 60% for LC grown cells, but only 47% for HC grown cells (Fig. 2F).

After exposure to growth PAR or growth PAR + UV for 30 min, PSII ETR showed little change compared with initial values, and decreased slightly after 60 min exposure. PSII ETR for LC was higher than for HC by 6–11% for all radiation treatments (Fig. 3A). After exposure to high PAR, the PSII ETR of LC cells decreased by 36%, and decreased even more by 43% for HC cells. PSII ETR showed a different response under high PAR + UV; LC cells decreased by 24%, while HC cells increased slightly by ~9%. (Fig. 3B).

After high PAR + UV exposure for 60 min, Φ_{PSII} dropped to around 0.18 for both LC and for HC grown cells. During 1 h of subsequent dark incubation, Φ_{PSII} gradually recovered to about half of initial levels, whether treated with an inhibitor of chloroplast translation, or not (Fig. 4A). Under a subsequent period under low light (13 W m^{-2}), to mimic the light regime at the bottom of the photic zone, the cells further recovered to near initial values for Φ_{PSII} for both CO_2 grown cells without inhibitor, but showed no further recovery for inhibitor treated samples (Fig. 4A). After PAR + UV exposure, σ_{PSII} of both LC and HC cells increased to around 680 A^2 PSII^{-1}. During the subsequent 1 h dark incubation σ_{PSII} decreased to 580 A^2 PSII^{-1} for LC grown cells and to 350 A^2 PSII^{-1} for HC grown cells (Fig. 4B). After subsequent 30 min low light incubation, σ_{PSII} of LC grown cells decreased further to 240 A^2 PSII^{-1}, and to 210 A^2 PSII^{-1} for HC grown cells, but for both CO_2 treatments treated with inhibitor, σ_{PSII} remained stable through the whole incubation period (Fig. 4B).

In a parallel experiment Φ_{PSII} decreased to around 0.13 for both CO_2 grown cells after 1 h high PAR + UV exposure (Fig. 5A). During subsequent incubation under low light (13 W m^{-2}) that simulated cells moving to a depth within the euphotic zone, Φ_{PSII} of both CO_2 grown cells increased in the first 45 min, and then slowly increased to reach saturation near initial values over the subsequent 45 min. LC was lower than HC for the whole period until the end of light incubation. For LC and HC cells that were incubated in the dark, Φ_{PSII} only increased slightly to ~0.23 at the end of incubation (Fig. 5A). The recovery rate of LC grown cells under low light was ~50% lower than for HC grown cells, after a high light treatment (Fig. 5B).

4. Discussion

It is difficult to generalize whether ocean acidification (OA) negatively or positively affects phytoplankton, since opposing results have been found [5]. The interactive effects of OA with other abiotic factors including light and nutrients have been suggested as possible explanations [8,36]. In addition species-specific differences could be the most important biotic factor that determines the responses of given phytoplankton to OA. For example, OA effects on the calcification of coccolithophores depended on the species investigated [37]. For centric diatoms, ocean acidification

preferentially stimulated the growth rate of larger species under moderate light levels [38], while synergistically lowering diatom photosynthesis and growth with UV or high PAR [8,15]. In the present study, we found that OA alleviates UV damage on photosystem II in a pennate diatom, by accelerating the repair rate [24] of UV-damaged PSII [39,40] under low light, with a possible benefit to the competitiveness of this diatom in the future ocean.

Interruption of CO_2 fixation usually inhibits the repair processes and increases the susceptibility of photosystem II to light [28], in part because CO_2 fixation lowers the net excitation pressure on PSII [42]. It is also proposed that the newly fixed carbon might be a resource for the repair of PSII, since newly synthesized organic compounds were found to be crucial in PSII repair processes [43,44]. Cells cultured at a projected future CO_2 level had higher photosynthetic activity [31], and the relative inhibition induced by UV radiation under HC was smaller, indicating that the higher CO_2 availability could alleviate UV inhibition [41].

σ_{PSII} is the functional absorption cross-section area of PSII, a measurement of the probability that a quantum initiates photochemistry in PSII [23]. In present study, σ_{PSII} showed different responses to PAR or UV radiation, though both can induce photoinactivation in PSII. σ_{PSII} decreased significantly after exposure to low or high PAR indicating that the cells could down-regulate their light capture in response to PAR alone [45]. In contrast, under PAR + UV treatment Φ_{PSII} decreased by ~1/3 as PSII reaction centers were destroyed [46] while the σ_{PSII} for remaining PSII increased proportionally by ~3-fold, indicating that *P. tricornutum* employs a lake model rather than puddle model [47] to transfer light energy from pigments to remaining active PSII.

The primary target in PSII during PAR or UV photo-damage is the D1 protein, which is replaced by *de novo* synthesized proteins during PSII repair [39]. Usually, the repair process is stimulated by low light due to a requirement for resources from photosynthesis, to produce subunits and reassemble PSII [25,48]. In this study, Φ_{PSII} increased slowly in the dark after PAR + UV exposure despite the presence or absence of chloramphenicol, while after moving to growth light, Φ_{PSII} of non-chloramphenicol treated samples increased sharply, but Φ_{PSII} of chloramphenicol cells stayed a level similar to the end of dark period. That indicated photosynthetic products were essential for the full recovery of UV-damaged PSII unit [44]. The σ_{PSII} of non-chloramphenicol samples decreased in the dark, which indicated that some down-regulated antenna units recovered in the dark, and functioned again to deliver energy to PSII.

The LC and HC grown cells had similar photochemical yields after 1 h PAR + UV exposure, but showed significant differences in the recovery phase under low light (Fig. 4). HC grown cells recovered faster than LC indicating that the recovery of UV-damaged PSII can be stimulated by CO_2 in the presence of low light. Though LC cells finally achieved recovery similar to HC cells after 110 min low light exposure, the faster recovery of HC cells at the beginning of the recovery period has significant implications in the turbulent ocean, since time at deep water, under low light without detrimental UV radiation, is limited due to physical mixing. Therefore, diatoms under OA scenario should benefit from faster recovery of PSII under regimes of fluctuating light [20].

The present study shows that the increased CO_2 mitigated the UV detrimental effects on pennate diatom photosystem II, and facilitated the recovery process after UV-damage under low light. As previous studies have shown that ocean acidification also could synergistically increase the negative effects of UV radiation on centric diatom or phytoplankton assemblages [15,16], in the future ocean, increased CO_2 and UV radiation exposure could selectively favor some species against others, which could alter the dominant phytoplankton species, with functional implications to marine ecosystems [49].

Acknowledgements

K.G. was supported by National Natural Science Foundation of China (NSFC, No. 41120164007), Joint project of NSFC and Shandong province (Grant No. U1406403) and Strategic Priority Research Program of CAS (Grant No. XDA11020302). Y.W. was supported by National Natural Science Foundation of China (No. 41206091). D.C. was supported by Canada Research Chair Program.

Reference

[1] J. Beardall, C. Sobrino, S. Stojkovic, Interactions between the impacts of ultraviolet radiation, elevated CO_2, and nutrient limitation on marine primary producers, Photochem. Photobiol. Sci. 8 (2009) 1257–1265.
[2] S.C. Doney, V.J. Fabry, R.A. Feely, J.A. Kleypas, Ocean acidification: the other CO_2 problem, Mar. Sci. 1 (2009) 169–192.
[3] P.G. Brewer, A short history of ocean acidification science in the 20th century: a chemist's view, Biogeosciences 10 (2013) 7411–7422.
[4] J.M. Guinotte, V.J. Fabry, Ocean acidification and its potential effects on marine ecosystems, Ann. N.Y. Acad. Sci. 1134 (2008) 320–342.
[5] K. Gao, E.W. Helbling, D.-P. Häder, D.A. Hutchins, Responses of marine primary producers to interactions between ocean acidification, solar radiation, and warming, Mar. Ecol. Prog. Ser. 470 (2012) 167–189.
[6] V.J. Fabry, B.A. Seibel, R.A. Feely, J.C. Orr, Impacts of ocean acidification on marine fauna and ecosystem processes, ICES J. Mar. Sci. J. Cons. 65 (2008) 414–432.
[7] J.C. Orr, V.J. Fabry, O. Aumont, L. Bopp, S.C. Doney, R.A. Feely, et al., Anthropogenic ocean acidification over the twenty-first century and its impact on calcifying organisms, Nature 437 (2005) 681–686.
[8] K. Gao, J. Xu, G. Gao, Y. Li, D.A. Hutchins, B. Huang, et al., Rising CO_2 and increased light exposure synergistically reduce marine primary productivity, Nat. Clim. Change. 2 (2012) 519–523.
[9] P.L. Munday, D.L. Dixson, J.M. Donelson, G.P. Jones, M.S. Pratchett, G.V. Devitsina, et al., Ocean acidification impairs olfactory discrimination and homing ability of a marine fish, Proc. Natl. Acad. Sci. 106 (2009) 1848–1852.
[10] C.E. Williamson, R.G. Zepp, R.M. Lucas, S. Madronich, A.T. Austin, C.L. Ballaré, et al., Solar ultraviolet radiation in a changing climate, Nat. Clim. Change. 4 (2014) 434–441.
[11] D.-P. Häder, E.W. Helbling, C.E. Williamson, R.C. Worrest, Effects of UV radiation on aquatic ecosystems and interactions with climate change, Photochem. Photobiol. Sci. 10 (2011) 242.
[12] M. Tedetti, R. Sempéré, Penetration of ultraviolet radiation in the marine environment. A review, Photochem. Photobiol. 82 (2006) 389–397.
[13] W.-D. Zhai, N. Zheng, C. Huo, Y. Xu, H.-D. Zhao, Y.-W. Li, et al., Subsurface pH and carbonate saturation state of aragonite on the Chinese side of the North Yellow Sea: seasonal variations and controls, Biogeosciences 11 (2014) 1103–1123.
[14] R.A. Feely, C.L. Sabine, J.M. Hernandez-Ayon, D. Ianson, B. Hales, Evidence for upwelling of corrosive"acidified" water onto the continental shelf, Science 320 (2008) 1490–1492.
[15] C. Sobrino, M.L. Ward, P.J. Neale, Acclimation to elevated carbon dioxide and ultraviolet radiation in the diatom *Thalassiosira pseudonana*: effects on growth, photosynthesis, and spectral sensitivity of photoinhibition, Limnol. Oceanogr. 53 (2008) 494–505.
[16] Y. Wu, K. Gao, Combined effects of solar UV radiation and CO_2-induced seawater acidification on photosynthetic carbon fixation of phytoplankton assemblages in the South China Sea, Chin. Sci. Bull. 55 (2010) 3680–3686.
[17] Y. Li, K. Gao, V.E. Villafañe, E.W. Helbling, Ocean acidification mediates photosynthetic response to UV radiation and temperature increase in the diatom *Phaeodactylum tricornutum*, Biogeosciences 9 (2012) 3931–3942.
[18] M.R. Lewis, E.P.W. Horne, J.J. Cullen, N.S. Oakey, T. Platt, Turbulent motions may control phytoplankton photosynthesis in the upper ocean, Nature 311 (1984) 49–51.
[19] J.J. Cullen, M.R. Lewis, The kinetics of algal photoadaptation in the context of vertical mixing, J. Plankton Res. 10 (1988) 1039–1063.
[20] P. Jin, K. Gao, V.E. Villafañe, D.A. Campbell, E.W. Helbling, Ocean acidification alters the photosynthetic responses of a coccolithophorid to fluctuating ultraviolet and visible radiation, Plant Physiol. 162 (2013) 2084–2094.
[21] E.W. Helbling, K. Gao, R.J. Gonccalves, H. Wu, V.E. Villafañe, Utilization of solar UV radiation by coastal phytoplankton assemblages off SE China when exposed to fast mixing, Mar. Ecol. Prog. Ser. 259 (2003) 59–66.
[22] K. Gao, Y. Wu, G. Li, H. Wu, V.E. Villafañe, E.W. Helbling, Solar UV radiation drives CO_2 fixation in marine phytoplankton: a double-edged sword, Plant Physiol. 144 (2007) 54–59.
[23] P.G. Falkowski, J.A. Raven, Aquatic Photosynthesis, Princeton University Press, 2013.
[24] D.A. Campbell, E. Tyystjärvi, Parameterization of photosystem II photoinactivation and repair, Biochim. Biophys. Acta BBA – Bioenerg. 2012 (1817) 258–265.
[25] E.-M. Aro, I. Virgin, B. Andersson, Photoinhibition of photosystem II. Inactivation, protein damage and turnover, Biochim. Biophys. Acta BBA – Bioenerg. 1143 (1993) 113–134.

[26] G. Renger, M. Völker, H.J. Eckert, R. Fromme, S. Hohm-Veit, P. Gräber, On the mechanism of photosystem II deterioration by UV-B irradiation, Photochem. Photobiol. 49 (1989) 97–105.
[27] J.P. Krall, G.E. Edwards, Relationship between photosystem II activity and CO_2 fixation in leaves, Physiol. Plant. 86 (1992) 180–187.
[28] S. Takahashi, N. Murata, Interruption of the Calvin cycle inhibits the repair of photosystem II from photodamage, Biochim. Biophys. Acta BBA – Bioenerg. 1708 (2005) 352–361.
[29] E. Granum, J.A. Raven, R.C. Leegood, How do marine diatoms fix 10 billion tonnes of inorganic carbon per year?, Can J. Bot. 83 (2005) 898–908.
[30] Z.V. Finkel, J. Beardall, K.J. Flynn, A. Quigg, T.A.V. Rees, J.A. Raven, Phytoplankton in a changing world: cell size and elemental stoichiometry, J. Plankton Res. 32 (2010) 119–137.
[31] Y. Wu, K. Gao, U. Riebesell, CO_2-induced seawater acidification affects physiological performance of the marine diatom *Phaeodactylum tricornutum*, Biogeosciences 7 (2010) 2915–2923.
[32] J.J. Cullen, M.P. Lesser, Inhibition of photosynthesis by ultraviolet radiation as a function of dose and dosage rate: results for a marine diatom, Mar. Biol. 111 (1991) 183–190.
[33] F.M.M. Morel, J.G. Rueter, D.M. Anderson, R.R.L. Guillard, Aquil: a chemically defined phytoplankton culture medium for trace metal studies, J. Phycol. 15 (1979) 135–141.
[34] G. Li, Studies on the relationships of solar ultraviolet radiation (UVR) and photosynthetic carbon fixation by phytoplankton assemblages from the South China Sea, Shantou University, 2009.
[35] A.B. Barnett, Fireworx 1.0. 3. Dalhousie University: Halifax, NS, Canada, 2007.
[36] C.J.M. Hoppe, C.S. Hassler, C.D. Payne, P.D. Tortell, B. Rost, S. Trimborn, Iron limitation modulates ocean acidification effects on Southern Ocean phytoplankton communities, PLoS ONE 8 (2013) e79890.
[37] G. Langer, G. Nehrke, I. Probert, J. Ly, P. Ziveri, Strain-specific responses of *Emiliania huxleyi* to changing seawater carbonate chemistry, Biogeosciences 6 (2009) 2637–2646.
[38] Y. Wu, D.A. Campbell, A.J. Irwin, D.J. Suggett, Z.V. Finkel, Ocean acidification enhances the growth rate of larger diatoms, Limnol. Oceanogr. 59 (2014) 1027–1034.
[39] S. Takahashi, M.R. Badger, Photoprotection in plants: a new light on photosystem II damage, Trends Plant Sci. 16 (2011) 53–60.
[40] P. Heraud, J. Beardall, Changes in chlorophyll fluorescence during exposure of *Dunaliella tertiolecta* to UV radiation indicate a dynamic interaction between damage and repair processes, Photosynth. Res. 63 (2000) 123–134.
[41] H. Gong, S. Nilsen, J.F. Allen, Photoinhibition of photosynthesis in vivo: Involvement of multiple sites in a photodamage process under CO_2- and O_2-free conditions, Biochim. Biophys. Acta BBA – Bioenerg. 1142 (1993) 115–122.
[42] J.-D. Rochaix, Reprint of: regulation of photosynthetic electron transport, Biochim. Biophys. Acta BBA – Bioenerg. 2011 (1807) 878–886.
[43] A. Melis, Photosystem-II damage and repair cycle in chloroplasts: what modulates the rate of photodamage in vivo?, Trends Plant Sci 4 (1999) 130–135.
[44] S. Takahashi, N. Murata, Glycerate-3-phosphate, produced by CO_2 fixation in the Calvin cycle, is critical for the synthesis of the D1 protein of photosystem II, Biochim. Biophys. Acta BBA – Bioenerg. 1757 (2006) 198–205.
[45] S. Ihnken, J.C. Kromkamp, J. Beardall, Photoacclimation in *Dunaliella tertiolecta* reveals a unique NPQ pattern upon exposure to irradiance, Photosynth. Res. 110 (2011) 123–137.
[46] I. Vass, L. Sass, C. Spetea, A. Bakou, D.F. Ghanotakis, V. Petrouleas, UV-B-induced inhibition of photosystem II electron transport studied by EPR and chlorophyll fluorescence. Impairment of donor and acceptor side components, Biochem. (Mosc.) 35 (1996) 8964–8973.
[47] D.M. Kramer, G. Johnson, O. Kiirats, G.E. Edwards, New fluorescence parameters for the determination of QA redox state and excitation energy fluxes, Photosynth. Res. 79 (2004) 209–218.
[48] K. Shelly, P. Heraud, J. Beardall, Interactive effects of PAR and UV-B radiation on PSII electron transport in the marine alga *Dunaliella tertiolecta* (chlorophyceae), J. Phycol. 39 (2003) 509–512.
[49] P.G. Falkowski, M.J. Oliver, Mix and match: how climate selects phytoplankton, Nat. Rev. Microbiol. 5 (2007) 813–819.